

# Strength of nanotubes, filaments and nanowires from sonication-induced scission\*

Y. Y. Huang, T. P. J. Knowles and E. M. Terentjev

Cavendish Laboratory, University of Cambridge  
JJ Thomson Avenue, Cambridge CB3 0HE, U.K.

## Abstract

We propose a simple model to describe the cavitation-induced breakage of mesoscale filaments during their sonication in solution. The model predicts a limiting length below which scission no longer occurs. This characteristic length is a function of the tensile strength and diameter of the filament, as well as the solvent viscosity and cavitation parameters. We show that the model predicts accurately experimental results for materials ranging from carbon nanotubes to protein fibrils, and discuss the use of sonication-induced breakage as a probe for the strength of nanostructures.

---

\*This work was supported by the IRC in Nanotechnology, the EPSRC, the Gates Foundation and St. John's College.

Measurements of the mechanical properties of nanostructures, and of their strength in particular, are an essential requirement for fundamental understanding of the possibilities and performance limits of materials which are based on such structures. Typically elastic modulus and strength measurements are performed through mechanical manipulation of individual nanostructures, for example using scanning probe techniques [1–8]; however, because of the challenges intrinsically associated with nanoscale mechanics, such measurements remain involved and very time consuming. In this paper, we examine the fragmentation of filamentous structures under sonication. Based on a coarse-grained model of this process, we discuss an alternative approach to probe the strength of elongated nanostructures such as carbon nanotubes, and show that the limiting length that such structures reach after prolonged sonication reports accurately on their effective breaking strength. Our results furthermore shed light on the effect of commonly used sonication treatments on nanostructured materials.

Sonication is widely implemented in the dispersion of nano- and meso-scale particles and filaments. The principal origin of the enhanced dispersion is the ultra-high shear rate attained during cavitation events. Cavitation takes place when a threshold energy density (estimated by ref. [9] to be of the order of  $\sim 10 \text{ W/cm}^2$ ) is exceeded by an acoustic compression wave. Recent experiments and theories highlight the extreme conditions reached during cavitation: in the vicinity of an imploding bubble shear strain rates up to  $\sim 10^9 \text{ s}^{-1}$  [10, 11] and local temperatures of up to 15000 K [12] can be reached. The sonication parameters, such as container geometry, acoustic power and pulsing rates, determine the frequency and spatial distribution of bubble creation and implosion events, and therefore govern the changes of the dispersion morphology with time.

When filaments or tubular particles are being sonicated, a number of studies have reported unwanted breakage of such particles even in chemically inert media. Studies

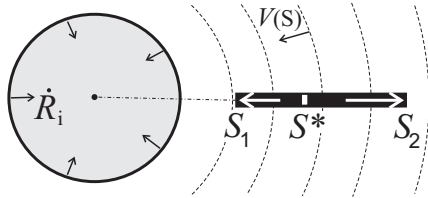


Figure 1: A scheme of cavitation bubble of radius  $R_i$  collapsing with a wall velocity  $\dot{R}_i$ . The instantaneous velocity field of the fluid at a distance  $S$  from the bubble center falls off with the inverse square of the distance:  $V(S) = R_i^2 \dot{R}_i / S^2$ . The points  $S_1$  and  $S_2$  denote the beginning and end positions of the filament of length  $L$ .

performed on carbon nanotubes (CNTs) [11, 13, 14] report that an initially broad length distribution of CNT lengths changes with sonication exposure: the mean CNT length gradually becomes shorter, finally reaching a constant modal length after prolonged sonication. The length distribution in the final steady-state has been found significantly narrower than in the initial population of filaments. This observation suggests that the reduction in filament length, for CNTs at least, was dominated by a mechanical/shearing process rather than a defect-mediated or random thermal/chemical breakdown (which would continue to occur without saturation). In this article we explore a simple theoretical argument for understanding the observed sonication-induced length reduction and eventual saturation at a given well-defined short length. We model the shear-induced scission (i.e. ultrasonication in a chemically inert medium) rather than the shortening accelerated by chemical effects [15]. This model predicts the existence of a limiting length of a filament, below which no further length reduction takes place at a given sonication power.

We consider a simple potential-flow description of bubble implosion dynamics which is based on the radial solvent flow around a bubble; within this framework we then use an affine estimate to calculate the stress that is exerted on a suspended filament by the viscous forces transmitted from the solvent. The key parameters describing this situation

are defined in Fig. 1. We consider a segment of the filament with a length  $L$  and a diameter  $d$ , which will be accelerated by the surrounding viscous (surface shear) forces. In a frame moving with the instantaneous velocity of the filament, the maximum net tensile stress will act at a point  $S^*$ , which is the fluid stagnation point on the filament surface. The value of this distance  $S^* = \sqrt{S_1 S_2}$ , as measured from the bubble center, can be found by balancing the tensile forces  $\eta \int_{S_1}^{S^*} V(s) - V(S^*) ds = -\eta \int_{S^*}^{S_2} V(s) - V(S^*) ds$  on both ends of the structure [16]. We can then evaluate the total tensile force pulling in each direction, and dividing this force by the cross-sectional area yields the maximal tensile stress  $\sigma_t$  exerted on the filament:

$$\sigma_t = \frac{8\eta}{d^2} R_i^2 \dot{R}_i \left[ \frac{1}{\sqrt{S_1}} - \frac{1}{\sqrt{S_1 + L}} \right]^2. \quad (1)$$

where  $\eta$  is the viscosity of the fluid in which the structures are suspended. For nanostructures with  $L \ll S_1$  i.e. with a length smaller than the size of a cavitation bubble, we can expand the square root in Eq. (1) to yield:  $\sigma_t = 2d^{-2}\eta R_i^2 \dot{R}_i S_1^{-3} L^2$ .

The tensile stress  $\sigma_t$  on the filament decreases dramatically as the filament length  $L$  diminishes, and a characteristic threshold length  $L_{\text{lim}}$  below which no scission would occur exists, when the stress is no longer sufficient to induce fragmentation. The maximal stress occurs for a filament positioned such that  $S_1 = R_i$  (Fig.1) and therefore we can write the tensile strength  $\sigma^*$  as a function of the limiting length  $L_{\text{lim}}$ :

$$L_{\text{lim}} = \sqrt{\frac{d^2 \sigma^*}{2\eta(\dot{R}_i/R_i)}}. \quad (2)$$

Strictly, Eqs.(1) and (2) are only applicable to low-viscosity solvents, as for higher viscosities the probability of cavitation is diminished and ultrasound energy absorption is increased. For the case of low viscosity  $\eta$ , it is convenient to further simplify the equation, by generically assuming similar  $R_i \sim 10 \mu\text{m}$ ,  $\dot{R}_i/R_i \sim 10^8 \text{ s}^{-1}$  values from the

literature [10, 11] and  $\eta \sim 0.01$  Pa.s for a typical low-molecular weight solvent, as quoted above, yielding (in SI units):

$$L_{\text{lim}} \approx 7 \times 10^{-4} d \sqrt{\sigma^*}. \quad (3)$$

This is a reasonable approximation for sonication performed in general low viscosity solvents, provided that cavitation events take place and that the length of the structures is smaller than the size of the cavitation bubbles. We therefore suggest that sonication parameters such as pulsing rate, power level (exceeding cavitation threshold) and container geometry only affect the time at which  $L_{\text{lim}}$  is achieved.

We now apply this model to the breakage of filamentous nanostructures such as multi-walled carbon nanotubes (MWNTs), protein fibrils and silver rods. These materials are representative examples of, respectively, covalent, non-covalent and metallic nanostructures. They are assembled through very different mechanisms: for example CNTs are composed of concentrically rolled graphene sheets, and protein (amyloid) fibrils consist of an elongated stack of  $\beta$ -strands formed as a result of the aggregation of misfolded peptides. We note that all of our measurements were performed under conditions where the bulk external temperature of the solvent was kept constant at  $\sim 15$  °C using a cooling system, in order to avoid chemical degradation of the structures from prolonged sonication heating.

After 3 hr of sonication, the length of MWNTs (diameter 60-100 nm) was reduced to  $\sim 2$ -6  $\mu\text{m}$  as shown by scanning electron microscopy (SEM) in Fig. 2(A). This length range was minimally affected even after an additional 7 hr sonication, Fig. 2(A3), where the few remaining longer tubes were fragmented, whereas the shorter tubes remain with similar lengths. Assuming  $\sigma^* \sim 4$  GPa for CVD MWNTs [17], and considering the widths of the MWNTs, Eq.(3) gives  $L_{\text{lim}}$  for our tested MWNTs in the range of 3-5  $\mu\text{m}$ ,

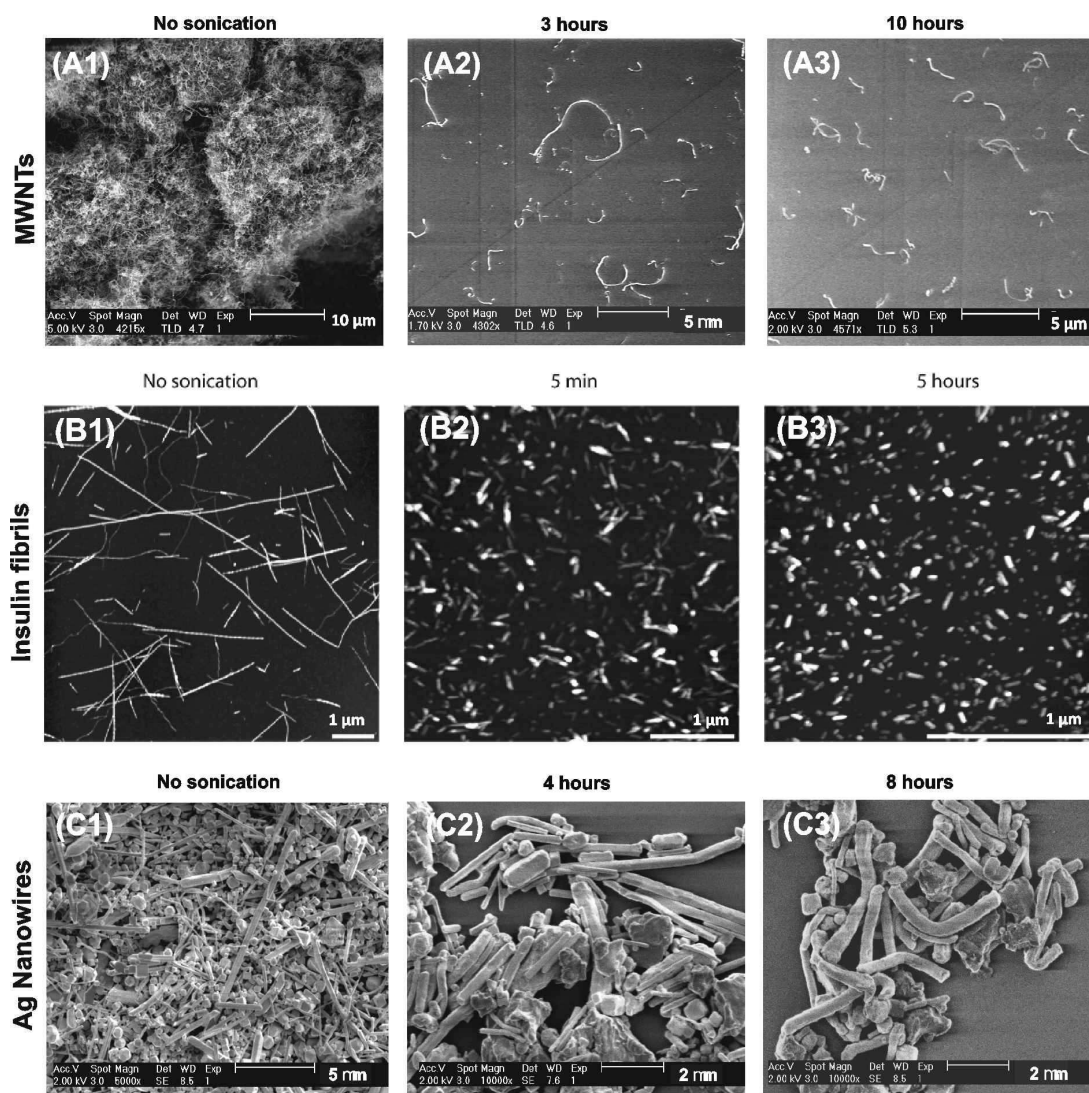


Figure 2: Micrographs of nanostructures before and after sonication. From top to bottom, A: scanning electron micrographs of MWNTs, B: atomic force micrographs of insulin amyloid fibrils, and C: silver nanowires.

in excellent agreement with the experimental observations in Fig. 2(A3). Note that we are not discussing here the kinetics of the dispersion process, as for instance the detailed study of [19]; we are testing the presence and the value of steady-state  $L_{\text{lim}}$ .

We next turn our attention to protein fibrils [20,21], formed here from bovine insulin under conditions which destabilize the native soluble state of the molecule and promote self-assembly into fibrillar nanostructures possessing diameters in the range of 3-6 nm and an as-grown length of several microns. Figure 2(B) show the atomic force micrographs (AFM) for the as-grown, 5 min sonicated, and 5 hr sonicated protein fibrils. The modal length of the fibrils was reduced by over a factor of 10 within the first 5 min of sonication; however, further sonication for up to 5 hrs only changed the modal length from 130 nm to 70 nm. It is noted that for insulin fibrils, effective cooling is of key importance for observing the existence of a limiting length. Sonication performed in the absence of temperature control frequently leads to complete degradation of structures and in some cases the formation of amorphous protein assemblies. The tensile strength of the protein fibrils has previously been estimated from AFM to be in the range 0.2-1.0 GPa [4]. Using the measured values for the diameter and strength range in Eq.(3), yields a value for  $L_{\text{lim}}$  between 29 and 130 nm, again in good agreement with the observations in Fig. 2(B3).

We finally probed the strength of silver nanowires (SNWs) by exposing them to prolonged sonication. The silver wires, as synthesized (Nanostructured & Amorphous Materials Inc, Houston USA) had lengths of 10-25  $\mu\text{m}$ ; after 4 hours of sonication, the length of the structures had been reduced to the range 1-6  $\mu\text{m}$  and after 8 hours no further reduction in length was observed, Fig. 2(C). The diameters of the silver wires exhibited significant variability, ranging from 100 to 600 nm. This system therefore provides a good basis for probing the validity of Eq. (2) which predicts a linear relationship between the diameter of nanoscale filaments and their terminal length under sonication induced scission.

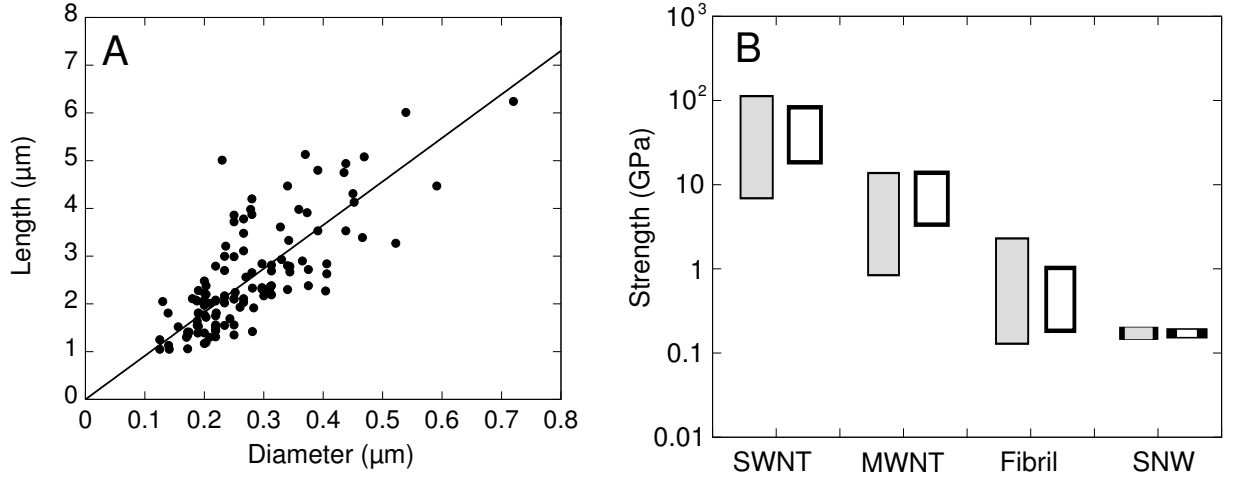


Figure 3: A: The terminal length of silver nanowires as a function of their diameter, fitted to Eq. (3). B: Comparison between literature values [2, 4, 11, 23, 24] for the strength of different nano-filaments (open boxes) and the values obtained in this study using Eq. (3) (filled boxes).

Figure 3A demonstrates that this linear dependence is very well satisfied; furthermore, we can extract an accurate estimate of the tensile strength  $\sigma^*$  of the material from the slope of the graph which is equal to  $L_{\text{lim}}/d = 7 \cdot 10^{-4} \sqrt{\sigma^*}$  resulting in  $\sigma^* = 1.69 \pm 0.04 \cdot 10^8$  Pa. This value is very close to the strength of bulk silver (170 MPa) [22].

The model was further tested against literature reports for single-wall carbon nanotubes (SWNTs) [11, 14] and MWNTs from ref. [13], and the largest difference between our estimate for  $L_{\text{lim}}$  and the measured modal length after scission was found to be a factor of two for the system of ref. [14]. This finding further supports our previous suggestion that the limiting length is only weakly dependent on sonication parameters, since all the experiments referenced above had employed different sonication settings.

Overall, it appears that Eq.(3) offers a very effective approximation, especially considering the simplicity of the model and the inevitably crude assumptions about the value of tensile strength  $\sigma^*$  for some of the cases. We do not exclude the presence of other mechanical failure mechanisms associated with cavitation. For example, differential



stress-induced bending failure might occur, which is not considered here. However, tensile failure is promoted since the sizes of the imploding bubbles ( $\sim 10$  s of microns) are of a similar scale or bigger than the length of typical filaments. The good agreement between the ultimate length observed in experiments, and the theoretical  $L_{\text{lim}}$  calculated based on literature values of the tensile strengths  $\sigma^*$  suggests that tensile failure is the dominant mechanism of fragmentation. The approach discussed in this paper therefore can form the basis for a practical evaluation of the tensile strength of different filaments from the extended sonication-scission experiments, without the need for micromanipulation of the individual structures. This idea is illustrated in Fig. 3B, which shows a comparison of the tensile strength of four different materials computed from their dimensions after sonication induced fragmentation, and existing values measured in mechanical experiments. In all cases the experimentally more straightforward length analysis yields tensile strength values in good /agreement with results from direct mechanical testing for different types of materials. The accuracy of our model prediction can be much increased if more precise values of solvent viscosity and cavitation parameters were to be used for each particular material.

In conclusion we have discussed a simple model which describes the fragmentation of elongated nanostructures under the action of hydrodynamic stresses imparted through sonication induced cavitation. We have shown that this model predicts the existence of a limiting length below which fragmentation no longer occurs. This length was furthermore shown to be highly dependent on the material properties of filaments, thereby opening up the possibility of using sonication-induced fragmentation as a sensitive probe of the strength of a range of materials in nano-filament form.

## Methods

A Cole Parmer 750 W ultrasonication system with a titanium tip was used in our study. The sonication tip pulsed at a 5 s on/3 s off interval, and the output power level was set at 25%, yielding an average power density of  $> 60 \text{ W/cm}^2$  for our container geometry, reliably exceeding the power density required for cavitation. The MWNTs studied here were obtained from Nanostructured & Amorphous Materials, Inc, grown by CVD, with a diameter range of 60-100 nm and as produced length between 5-15  $\mu\text{m}$ , Fig. 2(A1). Their dispersion in an organic solvent has been achieved with the help of pyrene-siloxane (PSi) surfactant synthesized in house. Amyloid fibrils (Bovine insulin, from Sigma Aldrich) were prepared by incubating the protein at 60C at the concentration of 10 mg/ml in water adjusted to pH=2 with HCl, as described elsewhere [21]. Silver Nanowires were purchased from Nanostructured & Amorphous Materials Inc (Houston USA), quoted grade ( $D = 270\text{-}330 \text{ nm}$ ,  $L = 10\text{-}25 \mu\text{m}$ ). Sonication and dispersion were performed in deionized water.

## References

- [1] M.F. Yu, O. Lourie, M.J. Dyer, K. Moloni, T.F. Kelly, & R.S. Ruoff, *Science*, **2000**, *287*, 637.
- [2] E.W. Wong, P.E. Sheehan, & C.M. Lieber, *Science*, **1997** *277*, 1971.
- [3] A. Kis, S. Kasas, B. Babić, A.J. Kulik, W. Benoît, G.A.D. Briggs, C. Schönenberger, S. Catsicas, & L. Forró, *Phys. Rev. Lett.* **2002**, *89*, 248101.
- [4] J.F. Smith, T.P.J. Knowles, C.M. Dobson, C.E. MacPhee, & M.E. Welland, *Proc. Natl. Acad. Sci. USA*, **2006**, *103*, 15806.

- [5] C. Durkan, A. Ilie, M.S.M. Saifullah, & M.E. Welland, *Appl. Phys. Lett.* **2002**, *80*, 4244.
- [6] J.P. Salvetat, G.A.D Briggs, J.M. Bonard, R.R. Bacsá, A.J Kulik, T. Stöckli, N.A Burnham, & L. Forró, *Phys. Rev. Lett.* **1999**, *82*, 944.
- [7] L. Yang, K.O. van der Werf, C.F.C. Fitié, M.L. Bennink, P.J. Dijkstra, & J. Feijen, *Biophys. J.* **2008**, *94*, 2204.
- [8] C. Guzmán, S. Jeney, L. Kreplak, S. Kasas, A.J. Kulik, U. Aebi, & L. Forró, *J. Mol. Biol.* **2006**, *360*, 623.
- [9] J.M. Pestman, J.B.F.N. Engberts, & F. Dejong, *J. Royal Netherlands Chem. Soc.* **1994**, *113*, 533.
- [10] T.Q. Nguyen, Q.Z. Liang, & H.H. Kausch, *Polymer*, **1997**, *38*, 3783.
- [11] F. Hennrich, R. Krupke, K. Arnold, J.A.R. Stütz, S. Lebedkin, T. Koch, T. Schimmel, & M.M. Kappes, *J. Phys. Chem. B*, **2007**, *111*, 1932.
- [12] D. Lohse, *Nature*, **2005**, *434*, 33.
- [13] J. Hilding, E.A. Grulke, Z.G. Zhang, & F. Lockwood, *J. Disp. Sci. Tech.* **2003**, *24*, 1.
- [14] J. Chun, J.A. Fagan, E.K. Hobbie, & B.J. Bauer, *Anal. Chem.* **2008**, *80*, 2514.
- [15] G.A. Forrest, & A.J. Alexander, *J. Phys. Chem. C*, **2007**, *111*, 10792.
- [16] S.V. Ahir, Y.Y. Huang, & E.M. Terentjev, *Polymer*, **2008**, *49*, 3841.
- [17] S.S. Xie, W.Z. Li, Z.W. Pan, B.H. Chang, & L.F. Sun, *J. Phys. Chem. Sol.* **2000**, *61*, 1153.

- [18] M.F. Yu, B.S. Files, S. Arepalli, & R.S. Ruoff, *Phys. Rev. Lett.* **2000**, *84*, 5552.
- [19] Y.Y. Huang, S.V. Ahir, & E.M. Terentjev, *Phys. Rev. B*, **2006**, *73*, 125422.
- [20] C.M. Dobson, (2003) *Nature*, **426**, 884.
- [21] T.P. Knowles, A.W. Fitzpatrick, S. Meehan, H.R. Mott, M. Vendruscolo, C.M. Dobson, & M.E. Welland, *Science*, **2007**, *318*, 1900.
- [22] A.M. Howatson, *Engineering Tables and Data* **1972**, Chapman and Hall, London, p.43.
- [23] J.P. Salvétat, J.M. Bonard, N.H. Thomson, A.J. Kulik, L. Forró, M. Benoit, & L. Zuppiroli, *Appl. Phys. A*, **1999**, *65*, 255.
- [24] F. Li, H.M. Cheng, S. Bai, G. Su & M.S. Dresselhaus, *Appl. Phys. Lett.* **2000**, *77*, 3161.